DMD Fast Forward. Published on December 29, 2020 as DOI: 10.1124/dmd.120.000215
This article has not been copyedited and formatted. The final version may differ from this version.

The Hypoglycemic Effect of Berberine and Berberrubine Involves Modulation of Intestinal FXR Signaling Pathway and Inhibition of Hepatic Gluconeogenesis

Runbin Sun[1], Bo Kong[2], Na Yang[4], Bei Cao[4], Dong Feng[1], Xiaoyi Yu[1], Chun Ge[1], Siqi Feng[1], Fei Fei[4], Jingqiu Huang[1], Zhenyao Lu[1], Yuan Xie[1], Chung S. Yang[3], Grace L. Guo[2], Guangji Wang[1,*] and Jiye Aa[1,*]

[1]Jiangsu Province Key Laboratory of Drug Metabolism and Pharmacokinetics, State Key Laboratory of Natural Medicines, China Pharmaceutical University, Nanjing, China, 210009

[2]Department of Pharmacology and Toxicology, Ernest Mario School of Pharmacy, Rutgers, The State University of New Jersey, Piscataway, New Jersey, United States of America, 08854

[3]Department of Chemical Biology, Ernest Mario School of Pharmacy, Rutgers, The State University of New Jersey, Piscataway, New Jersey, United States of America, 08854

[4]Nanjing Drum Tower Hospital, the Affiliated Hospital of Nanjing University Medical School, Nanjing, China, 210008

DMD Fast Forward. Published on December 29, 2020 as DOI: 10.1124/dmd.120.000215
This article has not been copyedited and formatted. The final version may differ from this version.

Running title: BBR and BRB Inhibited Gluconeogenesis through FXR

***Corresponding Authors:**

Jiye Aa, 24 Tongjiaxiang, Nanjing, China, 210009 (Address), (86)25-83271081 (phone), (86)25-83271060 (fax), Email: jiyea@cpu.edu.cn (e-mail)

Guangji Wang, 24 Tongjiaxiang, Nanjing, China, 210009 (Address), (86)25-83271081 (phone), (86)25-83271060 (fax), Email: guangjiwang@hotmail.com (e-mail)

Number of text pages: 38

Number of tables: 1

Number of figures: 7

Number of references: 58

Number of words in the Abstract: 235

Number of words in the Introduction: 736

Number of words in the Discussion: 1409

Abbreviations

AMPK, adenosine monophosphate-activated protein kinase; BBR, berberine; BCAAs, branched-chain amino acids; BSH, bile salt hydrolase; CYP7A1, cholesterol 7a-hydroxylase; d_4-CA, Cholic-2,2,4,4-d_4 Acid; d_4-TCA, Taurocholic-2,2,4,4-D_4 acid; d_4-GCA, Glycocholic-2,2,4,4-D_4 acid; DIO, diet-induced obese; FGF15/19, Fibroblast growth factor 15/19; FXR, Farnesoid X receptor; GC-MS, Gas Chromatography-Mass

DMD Fast Forward. Published on December 29, 2020 as DOI: 10.1124/dmd.120.000215
This article has not been copyedited and formatted. The final version may differ from this version.

Spectrometer; HFD, high fat diet; LDLR, low density lipoprotein receptor; M1, berberrubine; M2, thalifendine; M3, demethyleneberberine; M4, jatrorrhizine; NAFLD, non-alcoholic fatty liver disease; NASH, non-alcoholic steatohepatitis; OPLS-DA, orthogonal partial least squares discriminant analysis; Ostα, organic solute transporter alpha; PCA, principal components analysis; PCSK9, proprotein convertase subtilisin/kexin type 9; PLS-DA, partial least squares discriminant analysis; SHP, small heterodimer partner; SUS-plot, shared and unique structure-plot; TGR5, G protein-coupled bile acid receptor 1; VIP, variable importance in the projection.

DMD Fast Forward. Published on December 29, 2020 as DOI: 10.1124/dmd.120.000215
This article has not been copyedited and formatted. The final version may differ from this version.

Abstract

Our previous study suggests that berberine (BBR) lowers lipid by modulating bile acids and activating intestinal farnesoid X receptor (FXR). However, to what extent this pathway contributes to the hypoglycemia effect of BBR has not been determined. In this study, the glucose-lowering effects of BBR and its primary metabolites, berberrubine (M1) and demethyleneberberine (M3) in a high-fat diet-induced obese mouse model were studied, and their modulation on the global metabolic profile of mouse livers and the systemic bile acids were determined. The results revealed that BBR (150 mg/Kg) and M1 (50 mg/Kg) decreased mouse serum glucose levels by 23.15% and 48.14%, respectively. Both BBR and M1 markedly modulated the hepatic expression of genes involved in gluconeogenesis and metabolism of amino acids, fatty acids and purine. BBR showed a stronger modulatory effects on systemic bile acids than its metabolites. Moreover, molecular docking and gene expression analysis *in vivo* and *in vitro* suggest that BBR and M1 are FXR agonists. The mRNA levels of gluconeogenesis genes in the liver, glucose-6-phosphatase (*G6pase*) and phosphoenolpyruvate carboxykinase (*Pepck*), were significantly decreased by BBR and M1. In summary, BBR and M1 modulate systemic bile acids and activate the intestinal FXR signaling pathway, which reduces hepatic gluconeogenesis by inhibiting the gene expression of gluconeogenesis genes, and achieve a hypoglycemia effect. BBR and M1 may function as new natural intestinal specific FXR agonists with a potential clinical application to treat hyperglycemia and obesity.

Key words

DMD Fast Forward. Published on December 29, 2020 as DOI: 10.1124/dmd.120.000215
This article has not been copyedited and formatted. The final version may differ from this version.

Berberine, Berberubine, Hyperglycemia, FXR, bile acids, Gluconeogenesis

DMD Fast Forward. Published on December 29, 2020 as DOI: 10.1124/dmd.120.000215
This article has not been copyedited and formatted. The final version may differ from this version.

Significance Statement

This investigation revealed BBR and its metabolite, BRB, significantly lowered blood glucose, mainly through activating intestinal FXR signaling pathway directly by themselves or indirectly by modulating the composition of systemic bile acids, thus inhibited the expression of gluconeogenic genes in the liver, finally reduced hepatic gluconeogenesis and lowered blood glucose. The results will help elucidate the mechanism of BBR and provide a reference for mechanism interpretation of other natural products with low bioavailability.

DMD Fast Forward. Published on December 29, 2020 as DOI: 10.1124/dmd.120.000215
This article has not been copyedited and formatted. The final version may differ from this version.

Introduction

Obesity is now prevalent all over the world and causes at least 2.8 million deaths each year. Obesity is also the primary cause of various diseases, including type II diabetes, non-alcoholic fatty liver disease (NAFLD), cardiovascular disease, and hypertension. A common feature of these diseases is a metabolic disorder with abnormal glucose metabolism, lipids and amino acids (Gaggini et al., 2013; Yki-Järvinen, 2014). Berberine (BBR) is a compound isolated from plants such as *Coptis Chinensis* and *Hydrastis Canadensis* et al. and has been used for treating diseases including diarrhea, obesity, NAFLD and various tumors in both animal models and human because of its anti-microbial, antiprotozoal, antioxidant, anti-inflammatory and immune-modulatory properties (Yin et al., 2008; Zhang et al., 2008; Xing et al., 2011; Yu et al., 2015; Zou et al., 2017). BBR shows good anti-obesity and hypoglycemic effects through various mechanisms by stimulating glucose transport and uptake, increasing insulin receptor expression, enhancing gluconeogenesis and modulating glucose-6-phosphatase and hexokinase to achieve its hypoglycemic effect (Zhou et al., 2007; Zhang et al., 2010a; Xia et al., 2011; Li et al., 2014; Pirillo and Catapano, 2015). However, the mechanisms of BBR's actions are not fully understood. A large amount of BBR is accumulated in the gut after dosing due to its low bioavailability. Previous studies reported that the intestine might be the targeting organ for BBR's hypoglycemic effects, including inhibiting α-glucosidase, decreasing glucose transport through the intestinal epithelium, modulating the production of short-chain fatty acids (primarily butyrate) of the gut microbiota (Pan et al., 2003; Wang et al., 2017), and modulating

the composition of gut bacteria and the metabolism of bile acids as well (Gu et al., 2015; Sun et al., 2017).

BBR is extensively metabolized with oxidative demethylation followed by subsequent glucuronidation *in vivo* to various metabolites and the concentration of its metabolites in organs is higher than that of BBR in rats (Liu et al., 2010; Tan et al., 2013). Four primary Phase I metabolites of BBR have been identified, namely berberrubine (M1), thalifendine (M2), demethyleneberberine (M3) and jatrorrhizine (M4) in rats and humans (Qiu et al., 2008). The pharmacokinetic properties of metabolites exogenous given may be different with the metabolites generated endogenously (Prueksaritanont et al., 2006); thus we studied the pharmacokinetic property of M1 (Zhao et al., 2017b). Our previous study showed that M1 might have a much greater system exposure than BBR after oral administration in rats, and M1 had a more substantial glucose-lowering effect than BBR had, mainly by increasing glucose consumption, enhancing gluconeogenesis and stimulating the uptake of the glucose (Yang et al., 2016; Yang et al., 2017a). M3 can protect against non-alcoholic fatty liver disease by attenuating hepatic steatosis and fibrosis in mice mainly through suppressing NF-κB, activation of AMPK and inhibition of oxidative stress (Qiang et al., 2016; Wang et al., 2016). Moreover, the four metabolites of BBR can also up-regulate low-density lipoprotein receptor (LDLR) expression in human hepatoma cells (Zhou et al., 2014b). Based on all our previous findings, we hypothesized that the metabolites of BBR might also contribute to its anti-obesity and hypoglycemic activity.

DMD Fast Forward. Published on December 29, 2020 as DOI: 10.1124/dmd.120.000215
This article has not been copyedited and formatted. The final version may differ from this version.

Farnesoid X receptor (FXR) in the liver and intestine is critical in bile acid-mediated feedback suppression of bile acid synthesis and cholesterol metabolism. Besides the regulation of bile acid homeostasis, FXR activation also improved hyperglycemia and hyperlipidemia by decreasing hepatic gluconeogenesis and increasing glycogenesis (Schumacher and Guo, 2019), and ameliorate inflammation and fibrosis in NAFLD as well (Claudel et al., 2005; Ma et al., 2006; Adorini et al., 2012). However, non-selective activation of both hepatic and intestinal FXR presented some adverse effects with decreased HDL-C and increased LDL-C in the blood. Further studies suggest that intestine-specific FXR activation may be safer than whole-body FXR agonist for the treatment of metabolic syndrome, which leads to an increasing focus on the development of selective FXR modulators to achieve organ-specific FXR functions and reduction of side effects (Massafra et al., 2018). Our previous study showed that BBR could modulate the metabolism of bile acids and activate the intestinal FXR signaling pathway (Sun et al., 2017). However, the direct effect of BBR and its metabolites on FXR signaling pathway is still unclear. In this study, we determined the effect of BBR and its metabolites on bile acid metabolism, the direct and indirect action on intestinal FXR signaling pathway as well as the expression of *G6pase* and *Pepck* in the liver, and aimed to elucidate the mechanisms of their pharmacological effects.

DMD Fast Forward. Published on December 29, 2020 as DOI: 10.1124/dmd.120.000215
This article has not been copyedited and formatted. The final version may differ from this version.

Materials and Methods

Drug and reagents

BBR (≥98%) was purchased from Nanjing Zelang Medical Technology Co. Ltd. (Nanjing, China). M1 (≥95%) and M3 (≥95%) were synthesized by Nanjing Chemzam PharmTech Co. Ltd. (Nanjing, China). Methanol, chloroform, isopropanol and heptane were purchased from Merck KGaA (Darmstadt, Germany). Ethanol was purchased from Nanjing Chemical Reagent Co. Ltd. Millipore water was produced with a Milli-Q Reagent Water System (Millipore, MA, USA). Trizol kit was obtained from TaKaRa Biotechnology Co., Ltd. (Dalian, China). Myristic-1,2-$^{13}C_2$ acid was purchased from Cambridge Isotope Laboratories (Andover, MA, USA). Cholic-2,2,4,4-d_4 Acid (d_4-CA), Taurocholic-2,2,4,4-D_4 acid (d_4-TCA), Glycocholic-2,2,4,4-D_4 acid (d_4-GCA) were purchased from TLC PharmaChem (Concord, ON, Canada). Methoxyamine, pyridine and N-methyl-N-trimethyl-silyl-trifluoroacetamide (MSFTA) were purchased from Sigma-Aldrich (Shanghai, China).

Animal studies

Thirty-six male C57BL/6J mice (6 weeks old; obtained from Comparison Medical Center of Yangzhou University, Yangzhou, China) were fed with a standard chow diet (AIN-93M; containing 10% fat, 75.9% carbohydrate and 14.1% protein in total calories (3601 Kcal/Kg), Trophic Animal Feed High-Tech Co. Ltd, Nantong, China) and tap water *ad libitum*. They were housed at temperature and light controlled facility (temperature 25±2°C, relatively humidity (50±5%) and 12 h light/dark cycle

DMD Fast Forward. Published on December 29, 2020 as DOI: 10.1124/dmd.120.000215
This article has not been copyedited and formatted. The final version may differ from this version.

(06:00 a.m. to 6:00 p.m.) for one week to acclimate to the environment before the study.

To determine the effects of BBR, M1 and M3 on hyperglycemia and their anti-obesity activities, we weighed the mice and randomly divided them into six groups (n=6), as shown in Fig. S1. The vehicle group continued feeding with the standard diet, and the other groups were fed with a high-fat diet (HFD, Trophic Animal Feed High-Tech Co. Ltd, Nantong, China), which contains 60% fat, 25.9% carbohydrate and 14.1% protein in total calories (5018 Kcal/Kg), and 1% cholesterol to induce obesity and hyperglycemia. For intragastric administration, BBR, M1 and M3 were grounded and suspended in 0.5% CMC-Na aqueous solution to achieve a concentration of 15 mg/mL (150 mg/Kg of BBR), 2.5 mg/mL (25 mg/Kg of M1), 5 mg/mL (50 mg/Kg of M1) and 18 mg/mL (180 mg/Kg of M3), respectively, and the dose was 10 mL/Kg. All groups were weighed weekly and the food intake was recorded daily. After feeding for 7 weeks, the mice were placed in metabolic cages to collect feces. After administrated with BBR and its metabolites for another week, all mice were fasted overnight for 12 h and serum samples were collected and serum glucose levels were measured. Liver, ileum and cecal content were snap-froze in liquid nitrogen until molecular analyses were conducted. All animal experiments were performed with the approval of the Animal Ethics Committee of China Pharmaceutical University.

Metabolomics study

DMD Fast Forward. Published on December 29, 2020 as DOI: 10.1124/dmd.120.000215
This article has not been copyedited and formatted. The final version may differ from this version.

Metabolite profiling of mouse liver by Gas Chromatography-Mass Spectrometer (GC-MS)-based metabolomics method was described previously (A et al., 2005). Briefly, metabolites from 20 mg of liver tissue were extracted by 600 μL of 80% methanol (containing 5 μg/mL of myristic-1,2-$^{13}C_2$ acid as internal standard). An aliquot of 100 μL supernatant was transferred to a GC vial and dried by Savant SPD2010 Speedvac concentrator (Thermo Scientific, MA, USA). The extract was then oximated with 30 μL pyridine containing 10 mg/mL methoxyamine for 16 hr at room temperature, followed by derivatization with 30 μL MSTFA for 1 hr. Subsequently, 30 μL of heptane was added to the sample, and 0.5 μL sample was used to inject the Shimadzu QP2010Ultra/SE GC-MS system (Kyoto, Japan) with a RTx-5MS fused silica capillary column (30 m×0.25 mm ID, J&W Scientific, Bellefonte, PA, USA) at split mode.

Compound identification

The raw data acquired by GC-MS were processed by GCMS solution ver. 4.11 (Shimadzu Co., Kyoto, Japan), and the metabolites were identified by comparing the mass spectra and retention time of the detected peaks with NIST/EPA/NIH Mass Spectral Library (NIST14, National Institute of Standards and Technology, Gaithersburg, MD, USA) and Wiley Registry of Mass Spectral Data, 9th Edition (Wiley 9, John Wiley and Sons, Inc., Hoboken, New Jersey, USA) and an in-house mass spectra library database. The peak area of identified compounds in each sample was normalized to that of the internal standard.

Multivariate and univariate data analysis

DMD Fast Forward. Published on December 29, 2020 as DOI: 10.1124/dmd.120.000215
This article has not been copyedited and formatted. The final version may differ from this version.

SIMCA 13.0 software (Umetrices, Umeå, Sweden) was used to perform principal components analysis (PCA) and partial least squares discriminant analysis (PLS-DA). PCA model was used to check the overall distribution of all the samples, and the PLS-DA model was used to confirm the general separation among each group. The variable of importance in the projection (VIP) was used to identify the endogenous metabolites contributing to the classification. The strength of a pattern recognition model was evaluated by the parameters R^2X or R^2Y and Q^2Y parameters. Orthogonal partial least squares discriminant analysis (OPLS-DA) and shared and unique structure-plot (SUS-plot) was used to analyze the difference between two or three groups. Metabolomics pathway analysis of the metabolic biomarkers was carried out using MetaboAnalyst (www.metaboanalyst.ca) (Xia and Wishart, 2016).

Measurement of bile acids

The abundance of bile acids in serum, liver and feces were analyzed by LC-MS/MS (Shimadzu HPLC system coupled to an AB SCIEX 4000 mass spectrometer) as previously described (Zhou et al., 2014a; Sun et al., 2017). Briefly, bile acids were extracted with 70% ethanol containing d_4-GCA as an internal standard at 55°C for 4 h, and the extract was dried by Savant SPD2010 Speedvac concentrator (Thermo Scientific, MA, USA) and re-dissolved in 100 μL of 50% methanol-water. After centrifugation, 80 μL of supernatant was transferred to an LC vial and 10 μL was injected to a Waters Atlantis T3 column (2.1×100 mm, 3 μm) for chromatographic separation. The mobile phase consisted of solvent A (0.1% formic acid in water) and solvent B (methanol).

DMD Fast Forward. Published on December 29, 2020 as DOI: 10.1124/dmd.120.000215
This article has not been copyedited and formatted. The final version may differ from this version.

BSH activity measurement

Bile salt hydrolase (BSH) activity of the gut flora was measured as previously described (Zhao et al., 2014; Sun et al., 2017). The conversion of d_4-CA from d_4-TCA by BSH was analyzed by LC-MS/MS.

Quantitative real-time PCR

Total RNA from mouse liver, ileum and LS174T cells was extracted by Trizol reagent according to the manufacture's protocol, and reverse transcribed to cDNA by PrimeScript™ 1st Strand cDNA Synthesis kit were obtained from Takara Biotechnology (Dalian, China). The real-time PCR assay was performed using a SYBR-Green-based method (iTaq™ universal SYBR® Green supermix, Bio-Rad, Hercules, CA). The relative mRNA levels of all detected genes were normalized to that of β-actin in each sample (using the delta-delta Ct method). Results are expressed as fold change relative to the vehicle group, and primers used for the qPCR study were listed in Table 1.

Molecular docking

A computer-based modeling program (Autodock vina, USA) was employed to evaluate the binding of BBR and its metabolites with FXR. The chemical structures of BBR and its metabolites generated from PubChem (https://pubchem.ncbi.nlm.nih.gov), and the crystal structure of human FXR from Protein Data Bank (ID: 4WVD) (https://www.rcsb.org) were used for docking.

The effects of BBR and its metabolites on FXR signaling pathway *in vitro*

DMD Fast Forward. Published on December 29, 2020 as DOI: 10.1124/dmd.120.000215
This article has not been copyedited and formatted. The final version may differ from this version.

To investigate the effects of BBR, M1 and M3 on the activity of FXR and expression of *Fgf19*, LS174T cell (purchased from American Type Culture Collection, Manassas, VA) were plated in a 12 well plate at 1×10^5 per well. After 24 h, cells were treated with 0.1% DMSO (negative control), various concentrations of BBR (0.1 μM, 1 μM, 10 μM and 50 μM), M1 (0.1 μM, 1 μM, 10 μM and 100 μM), M3 (0.1 μM, 1 μM, 10 μM and 100 μM), and 100 μM of CDCA (positive control). Total RNA was isolated by Trizol Reagent (Takara, Dalian, China) 24 h after treatment gene expression level of *Fxr* and *Fgf19* were measured by real-time PCR. To test the effects of FXR antagonism by BBR and its metabolites, cells were treated 24 h with 100 μM of CDCA in the absence or presence of BBR and its metabolites or 0.1% DMSO as a negative control. Furthermore, the expression of *Fgf19* was determined after FXR was silenced with siRNA (5'-GAAUUCGAAAUAGUGGUAUCUCUGA-3', Invitrogen, Thermo Fisher Scientific) for 24 h and treated with BBR (25 μM), M1 (100 μM) and M3 (100 μM) for another 24 h.

Statistical analysis

All data are expressed as mean ± SD. Differences among groups were tested by one-way ANOVA followed by Fisher's LSD multiple comparison test and corrected by the Benjamini-Hochberg method to control the False Discovery Rate (FDR) (performed by R project, version 3.5.3). $P<0.05$ was considered statistically significant. The bar plots were generated by GraphPad Prism (Version 7.0).

DMD Fast Forward. Published on December 29, 2020 as DOI: 10.1124/dmd.120.000215
This article has not been copyedited and formatted. The final version may differ from this version.

Results

BBR and M1 protected mice against high-fat diet-induced obesity and hyperglycemia

There was no obvious difference in food intake among groups (Fig. S2). Comparing to mice on the control diet, the mice in the HFD group showed a significant increase in body weight (HFD group 31.79 ± 1.85 g vs. vehicle group 26.21 ± 1.68 g, $P<0.001$) and blood glucose levels (HFD group 12.17 ± 1.70 mmol/L vs. vehicle group 5.22 ± 2.34 mmol/L, $P<0.001$). BBR treatment protected the mice against diet-induced obesity (BBR group 28.16 ± 2.19 g vs. HFD group 31.79 ± 1.85 g, $P=0.011$, Fig. 1A) and hyperglycemia (BBR group 9.35 ± 1.60 mmol/L vs. HFD group 12.17 ± 1.70 mmol/L, $P=0.015$) (Fig. 1B). Oral administration of M1 also showed the protection from diet-induced obesity and hyperglycemia at different doses (25 mg/mL group 28.89 ± 1.60 g, 50 mg/mL group 23.98 ± 1. 91 g vs. HFD group 31.79 ± 1.85 g, $P=0.011$, Fig. 1A) and hyperglycemia (25 mg/mL group 8.83 ± 2.03 mmol/L, 50 mg/mL group 6.31 ± 1.67 mmol/L vs. HFD group 12.17 ± 1.70 mmol/L, $P=0.015$) (Fig. 1B). However, oral administration of M3 did not affect diet-induced obesity or hyperglycemia (Fig. 1A, B).

GC-MS profiles of hepatic metabolites and differential compound analysis

The representative chromatography of each group was shown in Fig. 2A. After deconvolution, identification and quantitation, a total of 98 compounds were identified in the liver, including various amino acids, organic acids, amines, saccharides, purines and fatty acids. For an overview of the dataset, 6 groups were

DMD Fast Forward. Published on December 29, 2020 as DOI: 10.1124/dmd.120.000215
This article has not been copyedited and formatted. The final version may differ from this version.

separated by PLS-DA (R^2X (cum) = 0.339, R^2Y (cum) = 0.313 and Q^2 (cum) = 0.0963), and samples in each group clustered close to each other (Fig. 2B). The OPLS-DA of each treatment group and HFD group was performed followed. BBR and both doses of M1 showed a good effect on regulating of abnormal metabolism of the liver induced by HFD feeding (Fig. 3A-C). Surprisingly, M3 also showed an obvious modulation effect of metabolites in the liver although it showed no obvious hypoglycemic effect (Fig. 3D). The SUS-plot and univariate statistic test revealed that the glycogenic amino acids including alanine, glutamic acid, glutamine, isoleucine, valine, cysteine, proline and threonine elevated in the high-fat diet group. Fatty acids, including arachidonic acid and palmitic acid, are also elevated in the high-fat diet group. The metabolites in the TCA cycle, including fumaric acid and malic acid, also increased. The level of lactic acid decreased in the high-fat diet group. BBR significantly reversed the increase of these amino acids and fatty acids and increased lactic acid, fumaric acid and malic acid. The modulation effect of M1 was weaker than that of BBR, and M3 treatment even showed an opposite trend (Fig. 3E-H and Fig. 4). The concentrations of BBR and its metabolites in the liver were shown in Fig. S3.

BBR and its metabolites changed the composition of bile acids

Bile acids are the metabolites of cholesterol and physiological ligands of FXR. The bile acid profiles in serum, liver and feces were analyzed by the LC-MS/MS method, shown in Fig. 5. The composition of conjugated bile acids and free bile acids in the serum, liver and feces was changed by HFD feeding and medical treatment.

DMD Fast Forward. Published on December 29, 2020 as DOI: 10.1124/dmd.120.000215
This article has not been copyedited and formatted. The final version may differ from this version.

Specifically, in the high-fat diet group, the serum levels of conjugated bile acids showed a trend of decrease, and the levels of free bile acids significantly decreased (Fig. 5A, B). The levels of conjugated bile acids and free bile acids in the liver were both reduced after high-fat feeding (Fig. 5C, D). In the feces, the levels of conjugated bile acids and free bile acids were both elevated (Fig. 5E, F). BBR treatment increased the conjugated bile acids and reduced the free bile acids in serum and feces (Fig. 5A-F), which is consistent with our previous study (Sun et al., 2017). The high dose of M1 increased free bile acids in the liver (Fig. 5D) and the conjugated bile acids in the feces (Fig. 5E). The low dose of M1 (25 mg/Kg) and M3 (180 mg/Kg) showed no noticeable effect on the total conjugated and free bile acids. In conclusion, BBR and M1 both modulated the composition of system bile acids, and BBR showed a far stronger modulation effect than its metabolite (Fig. 5).

BBR inhibited the activity of BSH while M1 and M3 showed no effect

BSH activity indicates the capacity of gut microbiota for hydrolyzing conjugated bile acids to unconjugated bile acids. Consistent with our previous study (Sun et al., 2017), a significant decrease of d_4-CA production was observed after BBR treatment. However, M1 and M3 treatment had no apparent effect on the hydrolyzation of d_4-TCA to d_4-CA (Fig. 5G).

BBR and M1 activated intestinal FXR signaling pathway and repressed hepatic gluconeogenic gene expression

The intestinal FXR target genes of *Fgf15* and *Shp* were up-regulated after BBR administration but without significance. The expression of organic solute transporter

DMD Fast Forward. Published on December 29, 2020 as DOI: 10.1124/dmd.120.000215
This article has not been copyedited and formatted. The final version may differ from this version.

alpha (*Ostα*) was up-regulated significantly by M1. M3 had no apparent effect on the expression of *Fgf15*, whereas it increased the expression of *Shp* (Fig. 6A-D). In the liver, BBR or its metabolites did not change the expressions of hepatic FXR target genes. These results suggested BBR and M1 might activate the intestinal but not hepatic FXR signaling pathway. BBR and M1 treatment both up-regulated the expression of *Ldlr* and inhibited the expression of *G6pase* and *Pepck* in the liver, whereas M3 only reduced the expression of *Pepck* (Fig. 6E-L).

BBR and M1 acted as agonists of FXR

Computational molecular docking was used to predict the interaction between BBR and its metabolites with human FXR. BBR (-8.6 kcal/mol), M1 (-9.0 kcal/mol) and M3 (-8.3 kcal/mol) showed similar affinities as CDCA (-9.7 kcal/mol) (Fig. 7A, B). FGF19 is the human ortholog of mouse FGF15. In LS174T cells, BBR induced the expression of *Fgf19* at the concentration of 10 μM and 50 μM by 2.25 (P<0.01) and 4.99 folds (P<0.001), respectively (Fig. 7C). M1 induced the expression of *Fgf19* at the concentration of 1 μM, 10 μM and 100 μM by 1.22 (P<0.05), 1.33 (P<0.05) and 2.34 folds (P<0.001), respectively (Fig. 7D). M3 induced the expression of *Fgf19* only at the concentration of 100 μM by 2.54 folds (P<0.001) (Fig. 7E). To test the FXR antagonism effects for BBR, M1 and M3, cells were treated with physiological FXR ligands of CDCA followed by BBR and its metabolites. When used simultaneously, the two compounds of BBR and M1 both synergistically activated FXR (Fig. 7F). CDCA alone induced the expression of *Fgf19* by 7.61 folds, while co-treatment with BBR (25 μM) and M1 (100 μM) induced *Fgf19* gene expression by

DMD Fast Forward. Published on December 29, 2020 as DOI: 10.1124/dmd.120.000215
This article has not been copyedited and formatted. The final version may differ from this version.

14.04 and 12.34 folds, respectively. However, M3 showed no synergistic effects on the expression of *Fgf19* (Fig. 7F). The induced expression of *Fgf19* was weakened after BBR, M1 and M3 were treated and FXR was silenced (Fig. 7G, H).

DMD Fast Forward. Published on December 29, 2020 as DOI: 10.1124/dmd.120.000215
This article has not been copyedited and formatted. The final version may differ from this version.

Discussion

BBR has been reported to have glucose and lipid-lowering effects in humans and different animal models, and several studies have demonstrated that the mechanism involves the alteration of metabolic pathways in the liver (Xing et al., 2011; Z et al., 2014; Pirillo and Catapano, 2015; Yu et al., 2015; Zou et al., 2017). However, in our previous study using animal models, we found BBR accumulated in the intestine with much excretion in feces. In contrast, its primary metabolites, M1 and M3, reached a high concentration of hundreds ng/mL in the liver. This finding was also confirmed by another study (Tan et al., 2013). Therefore, we hypothesized that BBR or its metabolites might affect the expression of genes and pathways in the liver and/or intestine to lower serum glucose levels and reduce body weight.

The metabolomics of serum/plasma, urine, gut content/feces, and local tissues/organs had been studied after BBR treatment in obese or hyperglycemia and hyperlipidemia model in different species, and these studies showed that orally administered BBR leads to global change in metabolism including glycolysis, amino acid metabolism and lipid metabolism (Jiang et al., 2012; Li et al., 2015; Dong et al., 2016; Li et al., 2016). Because gluconeogenesis mainly takes place in the liver, and liver was regarded as the primary target organ for BBR in previous studies, the metabolomics of the liver was profiled to determine the modulatory effects of BBR and its metabolites on metabolism. After treatment with BBR or M1, the elevated levels of lactic acid and tricarboxylic acid cycle intermediates revealed acceleration in energy metabolism and glucose consumption. In contrast, decreased levels of amino

acids involved in glucogenesis (glutamic acid and branched-chain amino acids) were also observed. The reduced fatty acid levels suggest inhibition of synthesis or enhanced metabolism of lipids.

BBR can improve hepatic glucose and lipid metabolism in various metabolic diseases through multiple pathways. The underlying mechanisms may involve activation of adenosine monophosphate-activated protein kinase (AMPK), improvement of insulin sensitivity, and up-regulation of low-density lipoprotein receptor (LDLR) (Kong et al., 2004; Zhang et al., 2010b; Zhang et al., 2012; Wei et al., 2016; Zhao et al., 2017a). BBR could also increase glucose utilization in adipocytes and myocytes and decrease glucose transportation in intestinal cells by inhibiting α-glucosidase. Moreover, the expression of gluconeogenic genes and several lipid metabolism genes were modulated by BBR (Xia et al., 2011). A significant reduction in the *Pepck* and *G6pase* expression and a significant elevation in *Ldlr* expression in the livers of mice treated with BBR were observed, with the results consistent with previously published reports (Kong et al., 2004; Xia et al., 2011). Furthermore, in the livers of M1-treated mice, a similar trend of the expression of these genes was observed, which showed M1 also modulated gluconeogenesis even at a lower dose. We consider that these pathways may be the primary pathways responsible for the glucose-lowering effects of BBR and M1. However, whether these effects were the direct or indirect function of BBR and M1 still needs to be further investigated.

DMD Fast Forward. Published on December 29, 2020 as DOI: 10.1124/dmd.120.000215
This article has not been copyedited and formatted. The final version may differ from this version.

According to our previous study and several other studies, BBR may function through modulating the composition of gut bacteria, bile acids and intestinal signaling pathways (Zhang et al., 2012; Gu et al., 2015; Sun et al., 2017). Bile acids are endogenous ligands of FXR, and individual bile acids have differential effects on bile acid signaling (Song et al., 2015). Bile acids activate FXR with different efficacy (CDCA > DCA > CA), and the conjugated bile acids are less potent, whereas TβMCA, UDCA and LCA showed FXR antagonism activity (Yu et al., 2002; Michaela et al., 2015). We found that the concentration of most FXR agonists including CA and TCA in the feces were significantly inreased and the concentration of FXR antagonists including LCA and UDCA were reduced considerably. In contrast, the concentrations of bile acids in the serum and liver were rarely changed except elevated TCA in the serum; this was in accordance with our previous study (Sun et al., 2017). However, the effects of BBR metabolites were far weaker than that of BBR. The overall impact of BBR and M1 treatment trended towards intestinal FXR activation, which suggests BBR and M1 may activate the intestinal FXR signaling pathway by their FXR activation effect directly or a combined activation of FXR with endogenous bile acids. It has been reported that FXR agonists could repress the expression of *G6pase* and *Pepck* in the liver (Zhang et al., 2006a), and the inhibited expression of *G6pase* and *Pepck* by BBR and M1 may be due to activation of intestinal the FXR signaling pathway.

FXR activation can improve glucose and lipid metabolism, and FXR, especially intestinal-specific agonism of FXR, may be a potential target for treating obesity and

NASH (Zhang et al., 2006b; Potthoff et al., 2011; Adorini et al., 2012). Intestinal FXR-FGF15/19 pathway can regulate hepatic glucose metabolism, mainly by modulating the CREB-PGC-1α pathway and gluconeogenesis (Potthoff et al., 2011; Trabelsi et al., 2017). A phase III study of obeticholic acid (OCA®, INT-747) for treating NASH has been finished, with the results showing that the primary endpoint for improving liver fibrosis without worsening of NASH was reached (Zhang et al., 2009; Mudaliar et al., 2013; Neuschwander-Tetri et al., 2015). For natural compounds, epigallocatechin gallate (EGCG) and its analogs are found can activate FXR specifically and dose-dependently *in vivo* and *in vitro* (Li et al., 2012; Sheng et al., 2018). In this study, from molecular docking assay and target gene analysis in C57BL/6J mice and LS174T cells, we demonstrate that BBR and M1 may activate FXR signaling pathway both *in vivo* and *in vitro*. In BBR and M1 treated mice, intestinal but not hepatic FXR signaling pathway was activated, shown by increased expression of *Fgf15* and *Shp* in the ileum and inhibition of *Shp* in the liver. Molecular docking analysis suggests that BBR and its metabolite M1 had similar binding energy with that of CDCA. We further validated the activation function of BBR and its metabolites on FXR by targeting gene analysis. These results all suggest that BBR and M1 may be agonists of the intestinal FXR signaling pathway. What's more, BBR and M1 can also enhance the activation effect of CDCA on FXR. We previously found BBR can modulate the composition of bile acids, and the elevated TCA in the intestine activates the intestinal FXR signaling pathway and lowering lipids in the liver (Sun et al., 2017). Here we found BBR treatment increases the levels of bile

acids which were FXR agonists and decrease the levels of bile acids which were FXR antagonists. In contrast, the modulation effect of M1 and M3 on bile acid metabolism is far weaker than that of BBR. These results suggest that the intestinal specific activation of FXR signaling pathway by BBR and M1 may be responsible for their glucose-lowering effect. BBR showed agonism effect on FXR *in vitro* directly, and the modulated composition of bile acids mediated by gut bacteria may enhance these effects. M1 showed a weaker agonism effect on FXR than BBR *in vitro* at the same dose, whereas it showed a stronger effect on anti-obesity and hypoglycemia in C57BL/6J mice at a lower dose, this difference may be because the fact that the bioavailability of M1 is better than that of BBR, as shown in our previous study (Yang et al., 2017b; Zhao et al., 2017b). The role of M1 itself may have been dominant for its hypoglycemic effect independent of bile acids. Our findings may provide new natural intestinal specific FXR agonists which are potential for the treatment of hyperglycemia and NASH.

In conclusion, we found BBR and M1 could ameliorate obesity and hyperglycemia induced by high-fat diet feeding, and M1 was even more effective than BBR. BBR and M1 could modulate several metabolic pathways in the liver of C57BL/6J mice. The combined *in vivo* and *in vitro* data showed BBR and its metabolite M1 are FXR agonists. The activation of the intestinal FXR signaling pathway by BBR and the modulated composition of bile acids may work together to achieve its pharmacological effects. However, the impact of M1 may be bile acid independent; it activated the intestinal FXR signaling pathway directly and repressed

DMD Fast Forward. Published on December 29, 2020 as DOI: 10.1124/dmd.120.000215
This article has not been copyedited and formatted. The final version may differ from this version.

the expression of hepatic gluconeogenesis genes with higher systemic exposure. Overall, BBR and M1 could activate the intestinal FXR signaling pathway, inhibit the expression and function of *G6pase* and *Pepck* in the liver thus reduce hepatic gluconeogenesis, and finally gain their glucose-lowering and anti-obeisty effect.

DMD Fast Forward. Published on December 29, 2020 as DOI: 10.1124/dmd.120.000215
This article has not been copyedited and formatted. The final version may differ from this version.

Authorship Contributions

Participated in research design: Jiye Aa, Guangji Wang, Grace L. Guo, Chung S. Yang and Runbin Sun

Conducted experiments: Runbin Sun, Bo Kong, Na Yang, Bei Cao, Dong Feng, Xiaoyi Yu, Chun Ge, Siqi Feng, Fei Fei and Zhenyao Lu

Performed data analysis: Runbin Sun, Jingqiu Huang

Contributed new reagents or analytic tools: Runbin Sun, Na Yang

Wrote and contributed to the writing of the manuscript: Runbin Sun, Bo Kong, Yuan Xie, Chung S. Yang, Grace L. Guo, Guangji Wang and Jiye Aa

References

A J, Trygg J, Gullberg J, Johansson AI, Jonsson P, Antti H, Marklund SL, and Moritz T (2005) Extraction and GC/MS analysis of the human blood plasma metabolome. *Analytical chemistry* **77:**8086-8094.

Adorini L, Pruzanski M, and Shapiro D (2012) Farnesoid X receptor targeting to treat nonalcoholic steatohepatitis. *Drug discovery today* **17:**988-997.

Claudel T, Staels B, and Kuipers F (2005) The Farnesoid X receptor: a molecular link between bile acid and lipid and glucose metabolism. *Arteriosclerosis, thrombosis, and vascular biology* **25:**2020-2030.

Dong Y, Chen YT, Yang YX, Zhou XJ, Dai SJ, Tong JF, Shou D, and Li C (2016) Metabolomics Study of Type 2 Diabetes Mellitus and the AntiDiabetic Effect of Berberine in Zucker Diabetic Fatty Rats Using Uplc-ESI-Hdms. *Phytotherapy Research Ptr* **30:**823-828.

Gaggini M, Morelli M, Buzzigoli E, DeFronzo RA, Bugianesi E, and Gastaldelli A (2013) Non-alcoholic fatty liver disease (NAFLD) and its connection with insulin resistance, dyslipidemia, atherosclerosis and coronary heart disease. *Nutrients* **5:**1544-1560.

Gu S, Cao B, Sun R, Tang Y, Paletta JL, Wu X-L, Liu L, Zha W, Zhao C, and Li Y (2015) A metabolomic and pharmacokinetic study on the mechanism underlying the lipid-lowering effect of orally administered berberine. *Molecular BioSystems* **11:**463-474.

Jiang Z, Liu F, Ong ES, and Li SFY (2012) Metabolic profile associated with glucose and cholesterol lowering effects of berberine in Sprague–Dawley rats. *Metabolomics* **8:**1052-1068.

Kong W, Wei J, Abidi P, Lin M, Inaba S, Li C, Wang Y, Wang Z, Si S, and Pan H (2004) Berberine is a novel cholesterol-lowering drug working through a unique mechanism distinct from statins. *Nature medicine* **10:**1344.

Li G, Lin W, Araya JJ, Chen T, Timmermann BN, and Guo GL (2012) A tea catechin, epigallocatechin-3-gallate, is a unique modulator of the farnesoid X receptor. *Toxicology and applied pharmacology* **258:**268-274.

Li J, Liu Z, Guo M, Xu K, Jiang M, Lu A, and Gao X (2015) Metabolomics Profiling to Investigate the Pharmacologic Mechanisms of Berberine for the Treatment of High-Fat Diet-Induced Nonalcoholic Steatohepatitis. *Evidence-Based Complementray and Alternative Medicine,2015,(2015-4-22)* **2015:**1-9.

Li M, Shu X, Xu H, Zhang C, Yang L, Zhang L, and Ji G (2016) Integrative analysis of metabolome and gut microbiota in diet-induced hyperlipidemic rats treated with berberine compounds. *Journal of Translational Medicine* **14:**237.

Li Z, Geng YN, Jiang JD, and Kong WJ (2014) Antioxidant and anti-inflammatory activities of berberine in the treatment of diabetes mellitus. *Evid Based Complement Alternat Med* **2014:**289264.

Liu YT, Hao HP, Xie HG, Lai L, Wang Q, Liu CX, and Wang GJ (2010) Extensive intestinal first-pass elimination and predominant hepatic distribution of

berberine explain its low plasma levels in rats. *Drug Metabolism & Disposition the Biological Fate of Chemicals* **38:**1779.

Ma K, Saha PK, Chan L, and Moore DD (2006) Farnesoid X receptor is essential for normal glucose homeostasis. *The Journal of clinical investigation* **116:**1102-1109.

Massafra V, Pellicciari R, Gioiello A, and van Mil SW (2018) Progress and challenges of selective Farnesoid X receptor modulation. *Pharmacology & Therapeutics*.

Michaela M, Anders T, Thierry C, Pooja J, Harald K, Carolin L, Bastian H, Guenter F, Tatjana S, and Curt E (2015) Ursodeoxycholic acid exerts farnesoid X receptor-antagonistic effects on bile acid and lipid metabolism in morbid obesity. *Journal of Hepatology* **62:**1398-1404.

Mudaliar S, Henry RR, Sanyal AJ, Morrow L, Marschall HU, Kipnes M, Adorini L, Sciacca CI, Clopton P, and Castelloe E (2013) Efficacy and safety of the farnesoid X receptor agonist obeticholic acid in patients with type 2 diabetes and nonalcoholic fatty liver disease. *Gastroenterology* **145:**574-582. e571.

Neuschwander-Tetri BA, Loomba R, Sanyal AJ, Lavine JE, Van Natta ML, Abdelmalek MF, Chalasani N, Dasarathy S, Diehl AM, and Hameed B (2015) Farnesoid X nuclear receptor ligand obeticholic acid for non-cirrhotic, non-alcoholic steatohepatitis (FLINT): a multicentre, randomised, placebo-controlled trial. *The Lancet* **385:**956-965.

Pan G-Y, Huang Z-J, Wang G-J, Fawcett JP, Liu X-D, Zhao X-C, Sun J-G, and Xie Y-Y (2003) The antihyperglycaemic activity of berberine arises from a decrease of glucose absorption. *Planta medica* **69:**632-636.

Pirillo A and Catapano AL (2015) Berberine, a plant alkaloid with lipid- and glucose-lowering properties: From in vitro evidence to clinical studies. *Atherosclerosis* **243:**449-461.

Potthoff MJ, Boney-Montoya J, Choi M, He T, Sunny NE, Satapati S, Suino-Powell K, Xu HE, Gerard RD, and Finck BN (2011) FGF15/19 regulates hepatic glucose metabolism by inhibiting the CREB-PGC-1α pathway. *Cell metabolism* **13:**729-738.

Prueksaritanont T, Lin JH, and Baillie TA (2006) Complicating factors in safety testing of drug metabolites: kinetic differences between generated and preformed metabolites. *Toxicology and applied pharmacology* **217:**143-152.

Qiang X, Xu L, Zhang M, Zhang P, Wang Y, Wang Y, Zhao Z, Chen H, Liu X, and Zhang Y (2016) Demethyleneberberine attenuates non-alcoholic fatty liver disease with activation of AMPK and inhibition of oxidative stress. *Biochemical & Biophysical Research Communications* **472:**603-609.

Qiu F, Zhu Z, Kang N, Piao S, Qin G, and Yao X (2008) Isolation and identification of urinary metabolites of berberine in rats and humans. *Drug Metab Dispos* **36:**2159-2165.

Schumacher JD and Guo GL (2019) Pharmacologic Modulation of Bile Acid-FXR-FGF15/FGF19 Pathway for the Treatment of Nonalcoholic Steatohepatitis. *Handbook of experimental pharmacology* **256:**325-357.

Sheng L, Jena PK, Liu H-X, Hu Y, Nagar N, Bronner DN, Settles ML, Bäumler AJ, and Wan Y-JY (2018) Obesity treatment by epigallocatechin-3-gallate–regulated bile acid signaling and its enriched Akkermansia muciniphila. *The FASEB Journal***:**fj. 201800370R.

Song P, Rockwell CE, Cui JY, and Klaassen CD (2015) Individual bile acids have differential effects on bile acid signaling in mice ☆. *Toxicology & Applied Pharmacology* **283:**57-64.

Sun R, Yang N, Kong B, Cao B, Feng D, Yu X, Ge C, Huang J, Shen J, and Wang P (2017) Orally administered berberine modulates hepatic lipid metabolism by altering microbial bile acid metabolism and the intestinal FXR signaling pathway. *Molecular pharmacology* **91:**110-122.

Tan XS, Ma JY, Feng R, Ma C, Chen WJ, Sun YP, Fu J, Huang M, He CY, and Shou JW (2013) Tissue Distribution of Berberine and Its Metabolites after Oral Administration in Rats. *Plos One* **8:**e77969.

Trabelsi MS, Lestavel S, Staels B, and Collet X (2017) Intestinal bile acid receptors are key regulators of glucose homeostasis. *The Proceedings of the Nutrition Society* **76:**192-202.

Wang Y, Shou JW, Li XY, Zhao ZX, Fu J, He CY, Feng R, Ma C, Wen BY, and Guo F (2017) Berberine-induced bioactive metabolites of the gut microbiota improve energy metabolism. *Metabolism Clinical & Experimental* **70:**72.

Wang Y, Zheng Z, Yan Y, Qiang X, Zhou C, Li R, Chen H, and Zhang Y (2016) Demethyleneberberine Protects against Hepatic Fibrosis in Mice by Modulating NF-κB Signaling. *International Journal of Molecular Sciences* **17:**1036.

Wei S, Zhang M, Yu Y, Lan X, Yao F, Yan X, Chen L, and Hatch GM (2016) Berberine Attenuates Development of the Hepatic Gluconeogenesis and Lipid Metabolism Disorder in Type 2 Diabetic Mice and in Palmitate-Incubated HepG2 Cells through Suppression of the HNF-4α miR122 Pathway. *Plos One* **11:**e0152097.

Xia J and Wishart DS (2016) *Using MetaboAnalyst 3.0 for Comprehensive Metabolomics Data Analysis*.

Xia X, Yan J, Shen Y, Tang K, Yin J, Zhang Y, Yang D, Liang H, Ye J, and Weng J (2011) Berberine improves glucose metabolism in diabetic rats by inhibition of hepatic gluconeogenesis. *PLoS one* **6:**e16556.

Xing L-J, Zhang L, Liu T, Hua Y-Q, Zheng P-Y, and Ji G (2011) Berberine reducing insulin resistance by up-regulating IRS-2 mRNA expression in nonalcoholic fatty liver disease (NAFLD) rat liver. *European journal of pharmacology* **668:**467-471.

Yang N, Sun R, Chen X, Zhen L, Ge C, Zhao Y, He J, Geng J, Guo J, and Yu X (2017a) In vitro assessment of the glucose-lowering effects of berberrubine-9-O-|[beta]|-D-glucuronide, an active metabolite of berberrubine. *Acta pharmacologica Sinica* **38:**351-361.

Yang N, Sun R, Zhao Y, He J, Zhen L, Guo J, Geng J, Xie Y, Wang J, and Feng S (2016) High fat diet aggravates the nephrotoxicity of berberrubine by

influencing on its pharmacokinetic profile. *Environmental Toxicology & Pharmacology* **46:**319-327.

Yang N, Sun RB, Chen XL, Zhen L, Ge C, Zhao YQ, He J, Geng JL, Guo JH, Yu XY, Fei F, Feng SQ, Zhu XX, Wang HB, Fu FH, Aa JY, and Wang GJ (2017b) In vitro assessment of the glucose-lowering effects of berberrubine-9-O-beta-D-glucuronide, an active metabolite of berberrubine. *Acta pharmacologica Sinica* **38:**351-361.

Yin J, Xing H, and Ye J (2008) Efficacy of berberine in patients with type 2 diabetes mellitus. *Metabolism-Clinical and Experimental* **57:**712-717.

Yki-Järvinen H (2014) Non-alcoholic fatty liver disease as a cause and a consequence of metabolic syndrome. *The lancet Diabetes & endocrinology* **2:**901-910.

Yu J, Lo JL, Huang L, Zhao A, Metzger E, Adams A, Meinke PT, Wright SD, and Cui J (2002) Lithocholic acid decreases expression of bile salt export pump through farnesoid X receptor antagonist activity. *Journal of Biological Chemistry* **277:**31441-31447.

Yu Y-N, Yu T-C, Zhao H-J, Sun T-T, Chen H-M, Chen H-Y, An H-F, Weng Y-R, Yu J, and Li M (2015) Berberine may rescue Fusobacterium nucleatum-induced colorectal tumorigenesis by modulating the tumor microenvironment. *Oncotarget* **6:**32013.

Z L, YN G, JD J, and WJ K (2014) Antioxidant and anti-inflammatory activities of berberine in the treatment of diabetes mellitus. *Evidence-Based Complementray and Alternative Medicine,2014,(2014-2-11)* **2014:**289264.

Zhang H, Wei J, Xue R, Wu J-D, Zhao W, Wang Z-Z, Wang S-K, Zhou Z-X, Song D-Q, and Wang Y-M (2010a) Berberine lowers blood glucose in type 2 diabetes mellitus patients through increasing insulin receptor expression. *Metabolism: clinical and experimental* **59:**285-292.

Zhang Q, Xiao X, Feng K, Wang T, Li W, Yuan T, Sun X, Sun Q, Xiang H, and Wang H (2010b) Berberine Moderates Glucose and Lipid Metabolism through Multipathway Mechanism. *Evid Based Complement Alternat Med* **2011:**: 924851.

Zhang S, Wang J, Liu Q, and Harnish DC (2009) Farnesoid X receptor agonist WAY-362450 attenuates liver inflammation and fibrosis in murine model of non-alcoholic steatohepatitis. *Journal of hepatology* **51:**380-388.

Zhang X, Zhao Y, Zhang M, Pang X, Xu J, Kang C, Li M, Zhang C, Zhang Z, and Zhang Y (2012) Structural changes of gut microbiota during berberine-mediated prevention of obesity and insulin resistance in high-fat diet-fed rats. *Plos One* **7:**e42529.

Zhang Y, Lee FY, Barrera G, Lee H, Vales C, Gonzalez FJ, Willson TM, and Edwards PA (2006a) Activation of the nuclear receptor FXR improves hyperglycemia and hyperlipidemia in diabetic mice. *Proceedings of the National Academy of Sciences* **103:**1006-1011.

Zhang Y, Lee FY, Barrera G, Lee H, Vales C, Gonzalez FJ, Willson TM, and Edwards PA (2006b) Activation of the nuclear receptor FXR improves hyperglycemia

and hyperlipidemia in diabetic mice. *Proceedings of the National Academy of Sciences of the United States of America* **103:**1006-1011.

Zhang Y, Li X, Zou D, Liu W, Yang J, Zhu N, Huo L, Wang M, Hong J, and Wu P (2008) Treatment of type 2 diabetes and dyslipidemia with the natural plant alkaloid berberine. *The Journal of Clinical Endocrinology & Metabolism* **93:**2559-2565.

Zhao C, Sun R, Cao B, Gu S, Zhao J, Liu L, Wang X, Zha W, Yu X, and Xiao W (2014) An in vitro metabolic system of gut flora and the metabolism of ginsenoside Rg3 and cholic acid. *European journal of drug metabolism and pharmacokinetics* **39:**129-137.

Zhao L, Zhen C, Sun H, Nie X, Wang N, and Lu Y (2017a) Berberine improves glucogenesis and lipid metabolism in nonalcoholic fatty liver disease. *Bmc Endocrine Disorders* **17:**13.

Zhao YQ, Yang N, Fei F, Sun RB, Feng SQ, He J, Huang JQ, Xie Y, Aa JY, and Wang GJ (2017b) Sensitive Analysis and Pharmacokinetic Study of Berberrubine Using LC-MS/MS. *Chinese Herbal Medicines* **9:**236-249.

Zhou L, Yang Y, Wang X, Liu S, Shang W, Yuan G, Li F, Tang J, Chen M, and Chen J (2007) Berberine stimulates glucose transport through a mechanism distinct from insulin. *Metabolism: clinical and experimental* **56:**405-412.

Zhou X, Cao L, Jiang C, Xie Y, Cheng X, Krausz KW, Qi Y, Sun L, Shah YM, Gonzalez FJ, Wang G, and Hao H (2014a) PPARalpha-UGT axis activation represses intestinal FXR-FGF15 feedback signalling and exacerbates experimental colitis. *Nature communications* **5:**4573.

Zhou Y, Cao S, Wang Y, Xu P, Yan J, Bin W, Qiu F, and Kang N (2014b) Berberine metabolites could induce low density lipoprotein receptor up-regulation to exert lipid-lowering effects in human hepatoma cells. *Fitoterapia* **92:**230-237.

Zou K, Li Z, Zhang Y, Zhang H-y, Li B, Zhu W-l, Shi J-y, Jia Q, and Li Y-m (2017) Advances in the study of berberine and its derivatives: a focus on anti-inflammatory and anti-tumor effects in the digestive system. *Acta pharmacologica Sinica* **38:**157.

DMD Fast Forward. Published on December 29, 2020 as DOI: 10.1124/dmd.120.000215
This article has not been copyedited and formatted. The final version may differ from this version.

Footnotes

This study was financially supported by the Key Technology Projects of China "Creation of New Drugs" (Grant number 2017ZX09301013), the National Natural Science Foundation of the People's Republic of China (Grant numbers 81573495, 81530098, 81703601, 81773814, 81421005), the Natural Science Foundation of Jiangsu Province (BK20190122), "Double First-Class" University project of China Pharmaceutical University (CPU2018GF01).

CONFLICT OF INTERESTS

The authors declare that there is no conflict of interest.

DMD Fast Forward. Published on December 29, 2020 as DOI: 10.1124/dmd.120.000215
This article has not been copyedited and formatted. The final version may differ from this version.

Legends for Figures

Figure 1. BBR and M1 prevented high-fat diet-induced weight gain and hyperglycemia in C57BL/6J mice.

A. Weekly body weight changes. B. Blood glucose. *, $P < 0.05$, **, $P < 0.01$, ***, $P < 0.001$, ****, $P < 0.0001$, compared with high-fat diet group, n=6.

Figure 2. Typical GC/MS chromatograms of all groups and the overview of the metabolomics data.

A. Typical GC/MS chromatograms of mouse liver from all groups. B. The scores plot of PCA showed that samples from vehicle group (Vehicle), high-fat diet group (HFD), 150 mg/Kg of BBR group (BBR), 25 mg/Kg of M1 group (M1-25), 50 mg/Kg of M1 group (M1-50) and 180 mg/Kg of M3 group (M3-180) were clustered separately.

Figure 3. The scores plot of PLS-DA analysis and SUS-plot of metabolite profile in the liver of C57BL/6J mice from all groups.

A. Scores plot of PLS-DA analysis of HFD, Vehicle and BBR group; B. Scores plot of PLS-DA analysis of HFD, Vehicle and M1-25 group; C. Scores plot of PLS-DA analysis of HFD, Vehicle and M1-50 group; D. Scores plot of PLS-DA analysis of HFD, Vehicle and M3-180 group; E, SUS-plot of metabolite profile in HFD, Vehicle and BBR group; F, SUS-plot of metabolite profile in HFD, Vehicle and M1-25 group; G, SUS-plot of metabolite profile in HFD, Vehicle and M1-50 group; H, SUS-plot of metabolite profile in HFD, Vehicle and M3-180 group.

DMD Fast Forward. Published on December 29, 2020 as DOI: 10.1124/dmd.120.000215
This article has not been copyedited and formatted. The final version may differ from this version.

Figure 4. Change of endogenous metabolites in the liver of C57BL/6J mice after BBR, M1 and M3 treatment for 8 weeks.

Gluconeogenesis pathway: Lactic acid; TCA cycle: Fumaric acid, Malic acid; Amino acids: Aspartic acid, Glutamic acid, Glutamine, Tryptophan, Phenylalanine, Proline, Alanine, Cysteine, Leucine, Isoleucine, Valine; Fatty acids: Arachidonic acid. *, $P < 0.05$, **, $P < 0.01$, ***, $P < 0.001$, ****, $P < 0.0001$, compared with high-fat diet group, n=6.

Figure 5. Changes in bile acid composition in the serum, liver and feces of C57BL/6J mice after BBR, M1 and M3 treatment.

Bile acids in serum, liver and feces were measured using LC-MS/MS. A, Change in total conjugated bile acids in the serum. B, Change in total free bile acids in the serum. C, Change in total conjugated bile acids in the liver. D, Change in total free bile acids in the liver. E, Change in total conjugated bile acids in the feces. F, Change in total free bile acids in the feces.(n=6). G, the production of d_4-CA by the gut microbiota of each group. *, $P < 0.05$, **, $P < 0.01$, ***, $P < 0.001$, compared with high-fat diet group, n=6.

Figure 6. BBR and M1 activated intestinal FXR signaling pathway but did not activate the hepatic FXR signaling pathway in C57BL/6J mice.

Relative mRNA levels of *Fxr* (A), *Fgf15* (B), *Shp* (C), and *Ostα* (D), in the distal ileum. Relative mRNA levels of *Fxr* (E), *Fgfr4* (F), *Shp* (G), *Cyp7a1* (H), *Bsep* (I), *Ldlr* (J), *G6pase*

DMD Fast Forward. Published on December 29, 2020 as DOI: 10.1124/dmd.120.000215
This article has not been copyedited and formatted. The final version may differ from this version.

(K), *and Pepck* (L), in the liver. *, $P < 0.05$, **, $P < 0.01$, compared with high-fat diet group, n=6.

Figure 7. BBR and M1 activated FXR signaling pathway in LS174T cells.

A, Structures of CDCA, BBR, M1 and M3. B, Molecular docking results of CDCA, BBR, M1 and M3 with human FXR. PCR analysis of LS174T cells after treatment with BBR (C), M1 (D) and M3 (E). F, the expression of *Fgf19* after co-treated with CDCA. The expression of *Fxr* (G) and *Fgf19* (H) after silenced by siRNA. *, $P < 0.05$, **, $P < 0.01$, ***, $P < 0.001$, comparison between BBR, M1 and M3 treated group with the corresponding control group. ##, $P < 0.01$, ###, $P < 0.001$, comparison between CDCA co-treated or siRNA silenced group with the corresponding untreated group. $, $P < 0.05$, $$, $P < 0.01$, comparison between BBR, M1 and M3 treated group with the corresponding groups cotreated with CDCA or silenced by siRNA.

DMD Fast Forward. Published on December 29, 2020 as DOI: 10.1124/dmd.120.000215
This article has not been copyedited and formatted. The final version may differ from this version.

Tables

Table 1. Primers used in qRT-PCR analysis.

Name	Primer sequence(5'-3')
Mouse-FXR-F	TCCGGACATTCAACCATCAC
Mouse-FXR-R	TCACTGCACATCCCAGATCTC
Mouse-FGF15-F	GAGGACCAAAACGAACGAAATT
Mouse-FGF15-R	ACGTCCTTGATGGCAATCG
Mouse-SHP-F	CGATCCTCTTCAACCCAGATG
Mouse-SHP-R	AGGGCTCCAAGACTTCACACA
Mouse-OSTα-F	GCCAGGCAGGACTCATATCAAA
Mouse-OSTα-R	GGCAACTGAGCCAGTGGTAAGA
Mouse-FGFR4-F	CAGGTCTGCCAAATCCTTGT
Mouse-FGFR4-R	CAGAGGCCTTTGGTATGGAT
Mouse-CYP7A1-F	AGCAACTAAACAACCTGCCAGTACTA
Mouse-CYP7A1-R	GTCCGGATATTCAAGGATGCA
Mouse-BSEP-F	CACACAAAGCCCCTACCAGT
Mouse-BSEP-R	CCAGAGGCAGCTATCAGGAC
Mouse-LDLR-F	AGGCTGTGGGCTCCATAGG
Mouse-LDLR-R	TGCGGTCCAGGGTCATCT
Mouse-G6Pase-F	GTGCAGCTGAACGTCTGTCTGTC
Mouse-G6Pase-R	TCCGGAGGCTGGCATTGTA
Mouse-PEPCK-F	GTGTTTGTAGGAGCAGCCATGAGA

DMD Fast Forward. Published on December 29, 2020 as DOI: 10.1124/dmd.120.000215
This article has not been copyedited and formatted. The final version may differ from this version.

Mouse-PEPCK-R	GCCAGTGGGCCAGGTATTTG
Mouse-β-actin-F	ATGGAGGGGAATACAGCCC
Mouse-β-actin-R	TTCTTTGCAGCTCCTTCGTT
Human-FXR-F	TGCATTGAAGTTGCTCTCAGGT
Human-FXR-R	CGCCTGACTGAATTACGGACA
Human-FGF19-F	CACGGGCTCTCCAGCTGCTTCCTGCG
Human-FGF19-R	TCCTCCTCGAAAGCACAGTCTTCCTCCG
Human-β-actin-F	GCGTGACATTAAGGAGAAG
Human-β-actin-R	GAAGGAAGGCTGGAAGAG

Figure 1

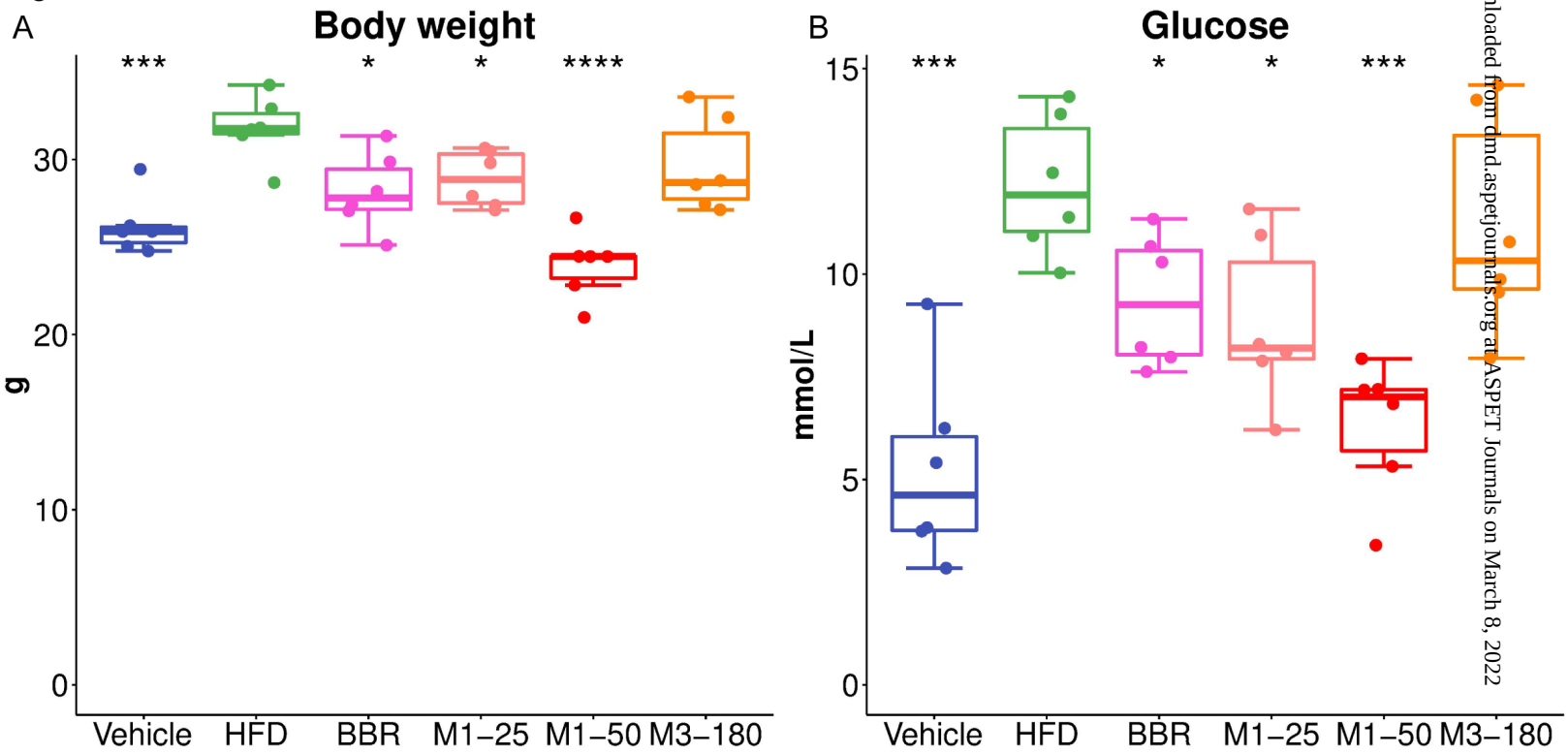

Figure 2

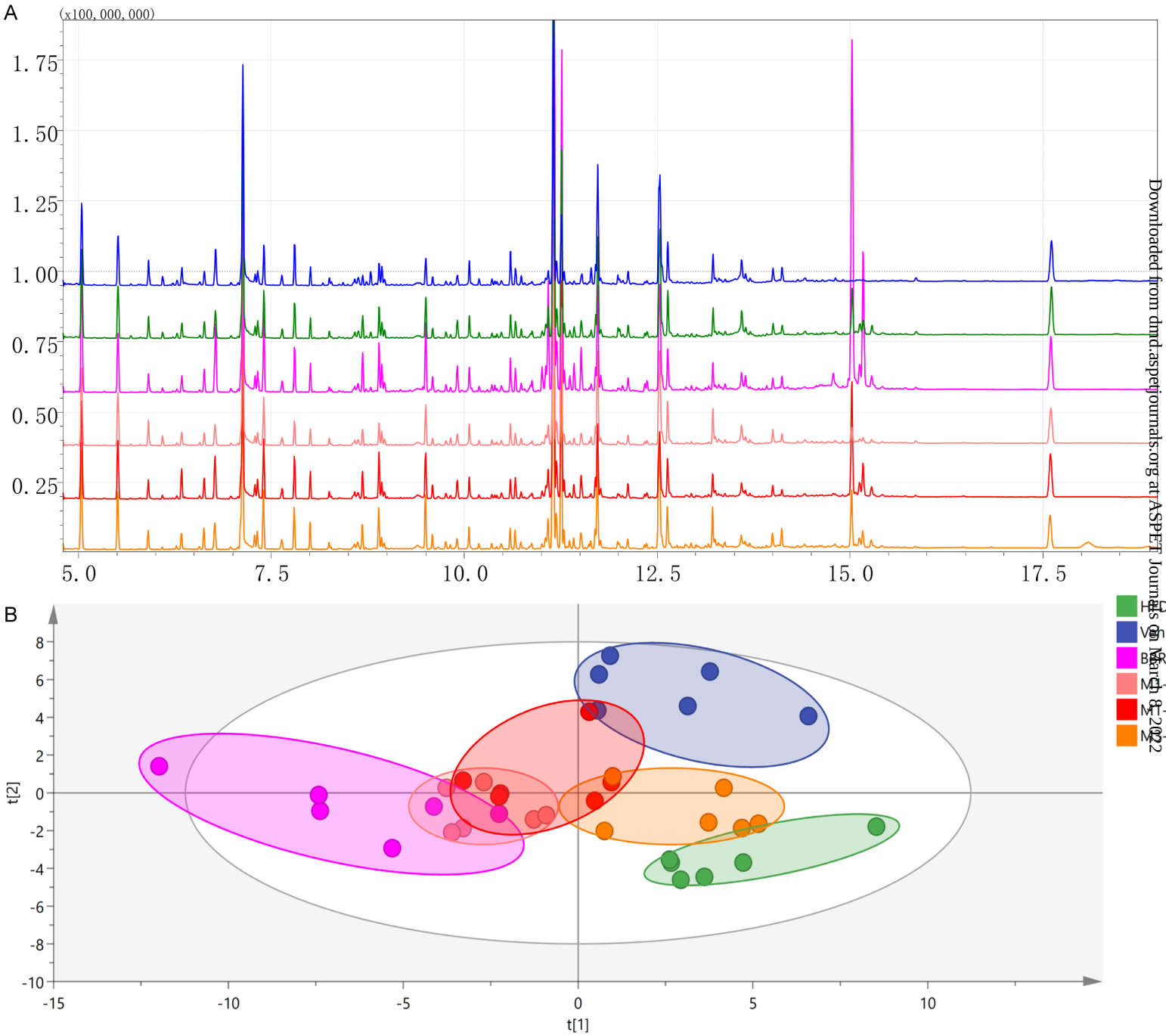

Figure 3

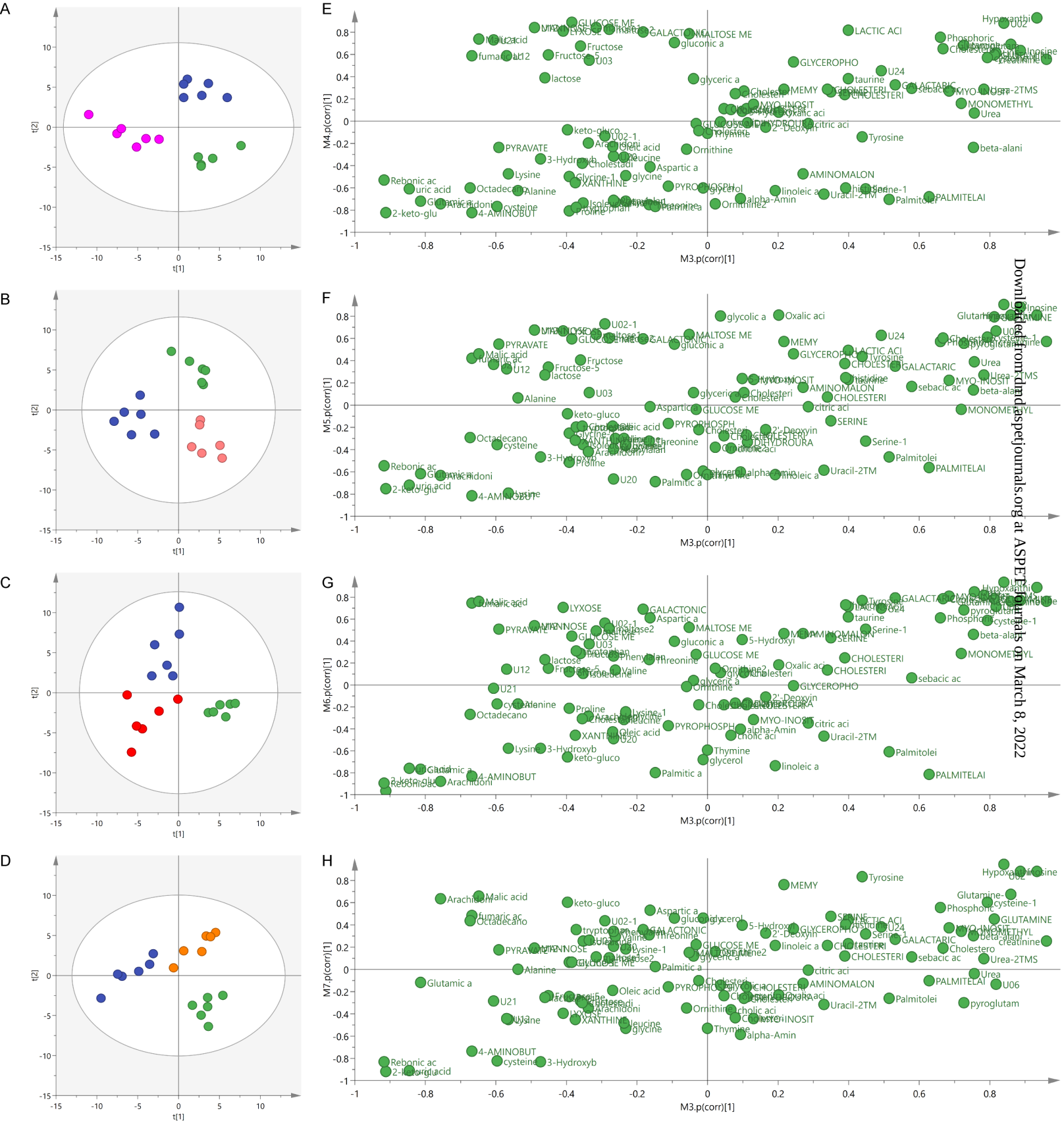

Figure 4

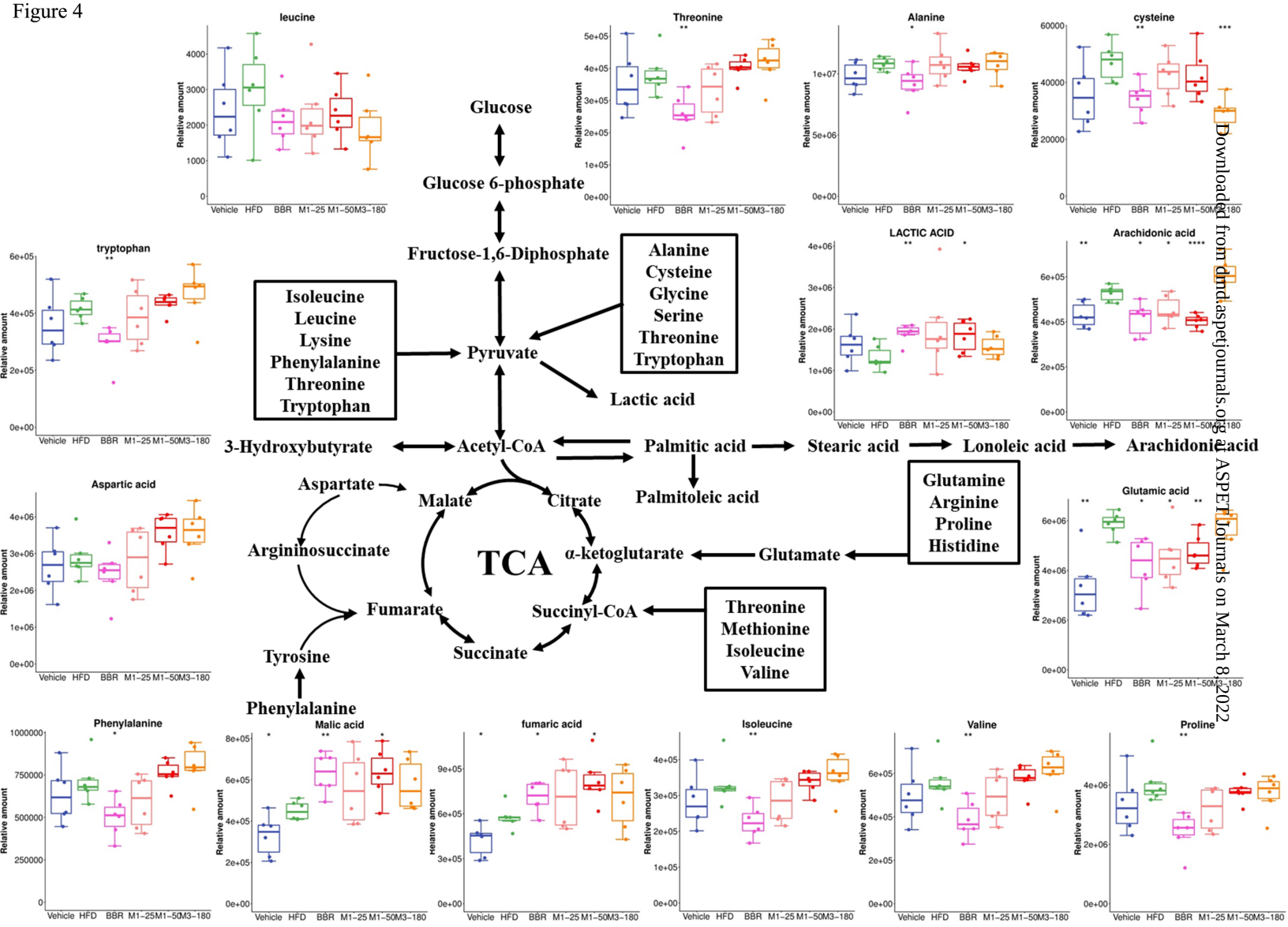

Figure 5

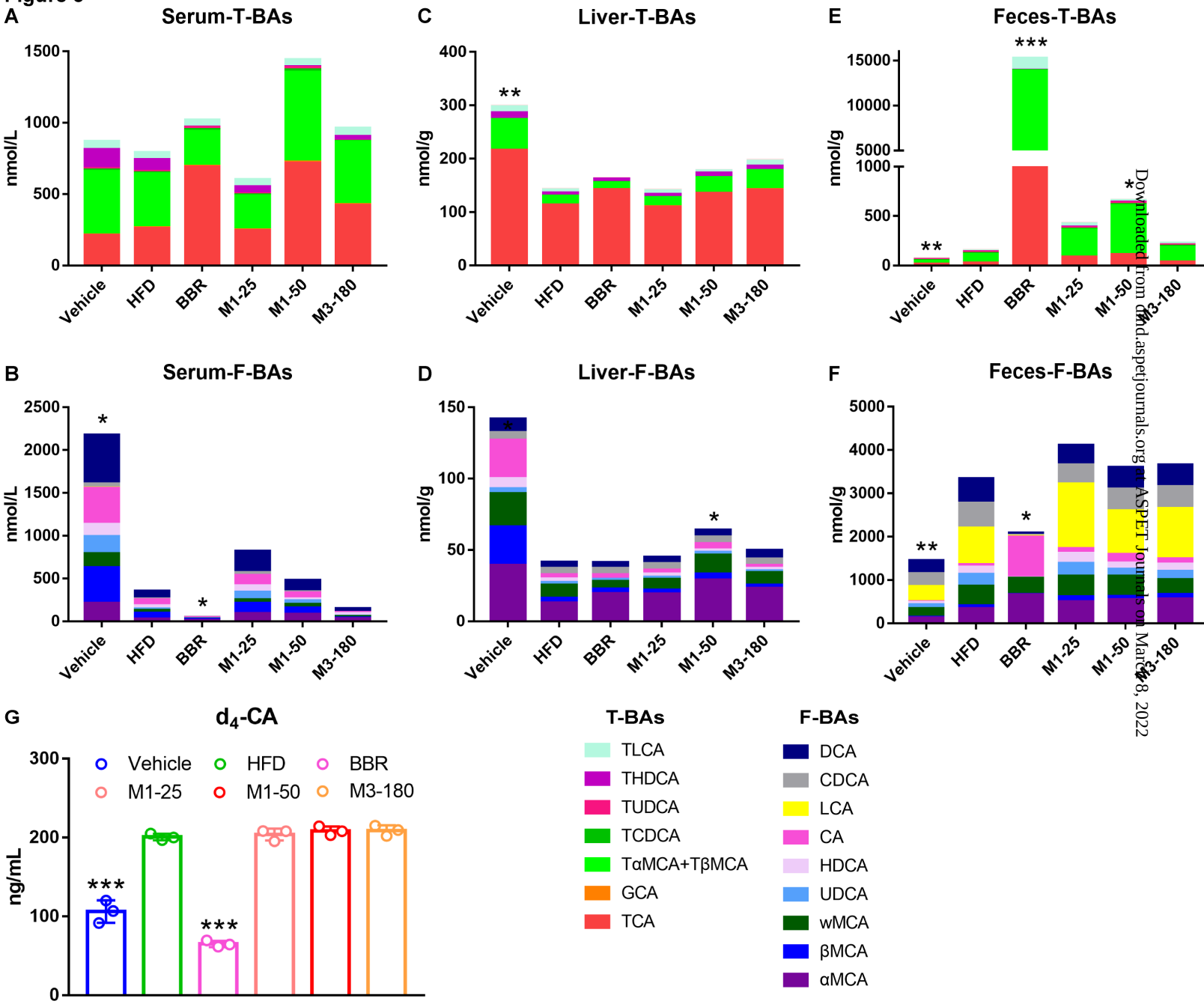

Figure 6

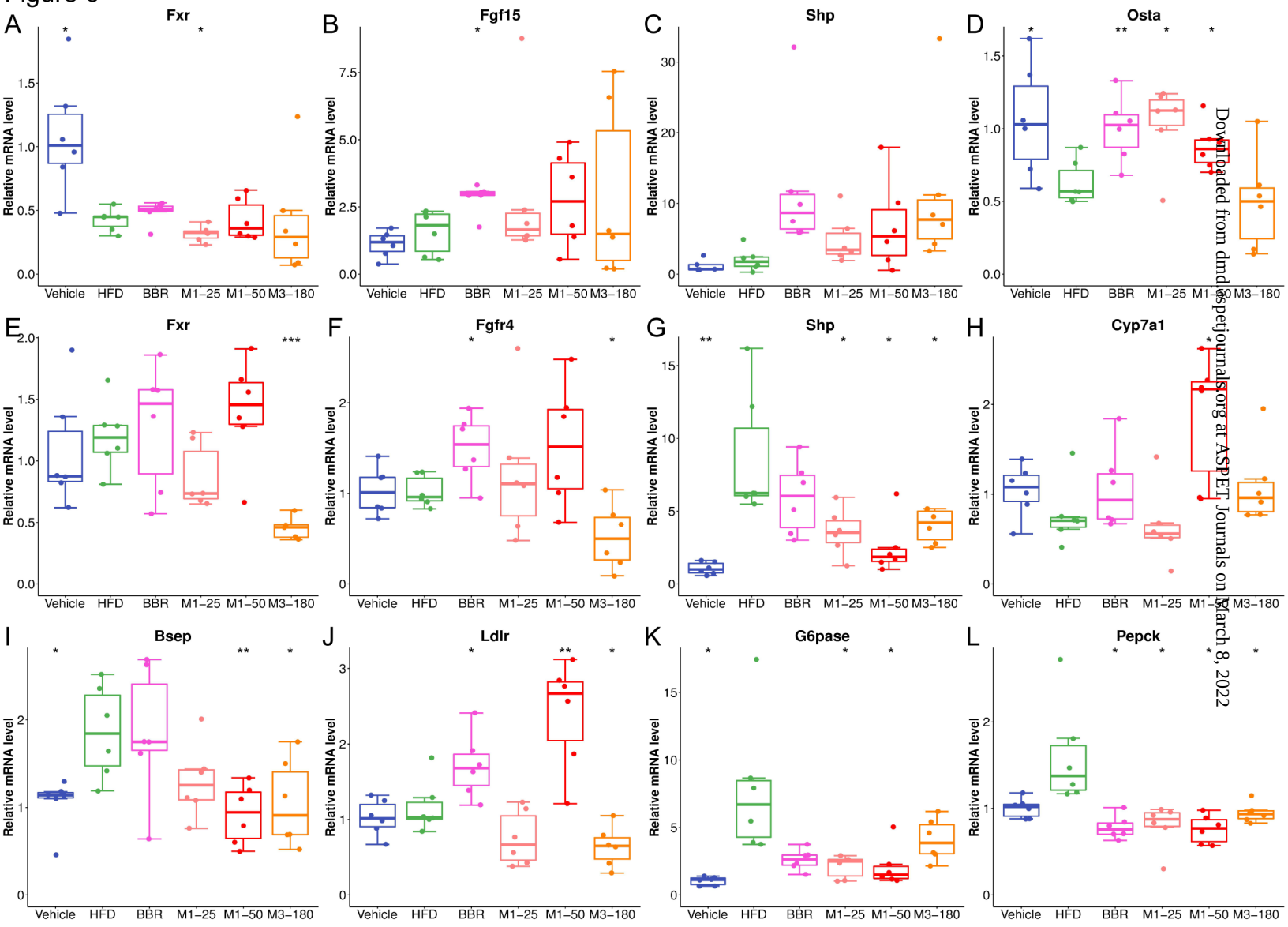

Figure 7